

Computer Model of Coronary Heart Disease


by

Colby Atkins
Bioengineering

Submitted in Partial Fulfillment of the
Requirements of the University Undergraduate
Fellows Program

1980-1981

Approved by:



G. E. MILLER

I would like to acknowledge the Honors Program for allowing me to participate in the University Undergraduate Fellows Program.

I wish to thank my advisor, Dr. Gerald E. Miller, for his patience and the amount of time he spent with me.

ABSTRACT - A computer code representing fluid flow is described which calculates the pressure gradient in the entry region of a rigid tube. The velocity profile is calculated from graphical correction of known flow equations. Poiseuille's model, a simplification of the z-momentum equation, is used as a basis for the calculations. The results obtained compare favorably with the literature.

INTRODUCTION

Atherosclerosis is responsible for greater than one-half of all deaths each year. Of these deaths, approximately two-thirds are a result of Coronary Heart Disease. Coronary Heart Disease is the degeneration of the coronary blood vessels, concluding with thrombotic events. Occlusion of the vessel leads to oxygen deprivation of the myocardium. Death generally occurs by myocardial infarction.

Atherosclerosis is principally a disease of the large arteries. Low density lipoproteins are transported across the blood vessel wall and deposited in the subintimal layer of the artery. The lipid deposits are known as atheromatous plaques. These plaques contain a high concentration of low density cholesterol.

If plaque build-up continues, the plaque will protrude through the intima into the flowing blood. An obstruction of the blood flow is termed a stenosis. A stenosis will generally lead to thrombosis. However, little is known about the origin of atherosclerosis.

Coronary Heart Disease is almost always a result of atherosclerosis. Diagnosis is usually made when a patient develops angina pectoris (with a stenosis) or myocardial infarction (with an occlusion). Angina pectoris, a cardiac pain, develops whenever the load on the heart becomes too great for the coronary blood flow to relieve.

Beyond an occluded vessel little or no blood flows. The now impaired cardiac muscle function is said to be infarcted. The overall process is termed myocardial infarction (4).

Hemodynamic factors probably play a decisive role in the progression of the stenosis. Severe stenoses

cause turbulence in the blood flow. It has been demonstrated that turbulence in the coronary arteries causes five times as much thrombus formation as does laminar flow(8). Additionally, arteries are distensible; if the stenosis creates a large pressure drop(Bernoulli's effect)the artery can collapse and thus expand the effective length of the stenosis(9). If turbulence is present, the pressure is even greater as energy is being expended to create the turbulence.

A pressure drop across a stenosis is more likely to occur than a reduction in flow rate. May and his colleagues found that there was no reduction in flow until the stenosis reached a critical value(for the iliac artery-85% by area, 62% by diameter)(7).

Stenoses also cause a jet stream through the constriction. By the Bernoulli effect the velocities of the blood particulates through the stenosis are highly accelerated.

A velocity profile is a plot of stream velocity versus radius for a vessel. Previously mentioned information outlining flow characteristics of atherosclerosis demonstrates the importance of the velocity profile in the diagnosis of the disease.

Presently, clinical methods of obtaining necessary data for blood flow are both painful and costly. Additionally, the limitations of these methods are great. For example, the present state-of-the-art clinical method for obtaining velocity profiles is Pulse Doppler Ultrasound(11). This device uses high frequency waves to sample points approximately 1 mm apart in a blood vessel. For the case of the left common coronary artery - diameter of 3 mm - only three points can be sampled. This is insufficient data to properly shape a profile. Thus, a model which could provide an accurate

profile would have great utility.

The objective of this project is to computer model a velocity profile, using published data for the coronary arteries.

On a gross scale, fluids are typically divided into two categories, perfect and viscous fluids. A perfect fluid is one whose viscosity is zero. A viscous fluid is one whose viscosity is non-zero and finite. Although a perfect fluid does not exist, low viscosity fluids such as air are often modeled as perfect. Blood is a viscous fluid. As a result, the remainder of this project is concerned with the development of viscous fluids.

Viscosity can be interpreted as a force - in particular a frictional force. When a viscous fluid enters a tube from a large reservoir its velocity profile is blunt. That is, all of its particulates have an equal velocity. As the fluid proceeds through the tube, a viscous drag shears the fluid. This drag occurs first at the wall, and progressively involves more and more layers up to the tube axis. At this point, the fluid is defined as fully developed. This term is interchangeable with Poiseuille flow. The velocity of the fluid at the wall equals zero; its shear rate is a maximum. The free stream velocity (the axis velocity) is a maximum and its shear rate equals zero.

The basic equations of viscous fluid mechanics are the Navier-Stokes equations.

For a cylindrical coordinate system, the Navier-Stokes equations are:

θ - direction

$$\rho \left[\frac{dV_{\theta}}{dt} + V_r \frac{dV_{\theta}}{dr} + \frac{V_{\theta}}{r} + \frac{V_r V_{\theta}}{r} + V_z \frac{dV_{\theta}}{dz} \right] = \rho g_{\theta} - \frac{1}{r} \frac{dP}{d\theta} + \mu \left[\frac{d}{dr} \left(\frac{1}{r} \frac{d}{dr} r V_{\theta} \right) + \frac{1}{r^2} \frac{\partial^2 V_{\theta}}{\partial \theta^2} + \frac{2}{r^2} \frac{\partial V_r}{\partial \theta} + \frac{\partial^2 V_{\theta}}{\partial z^2} \right] \quad (1)$$

R - direction

$$\rho \left[\frac{\partial V_r}{\partial t} + V_r \frac{\partial V_r}{\partial r} + \frac{V_\theta}{r} \frac{\partial V_r}{\partial \theta} - \frac{V_\theta^2}{r} + V_z \frac{\partial V_r}{\partial z} \right] = \rho g_r - \frac{dP}{dr} + \mu \left[\frac{\partial}{\partial r} \left(\frac{1}{r} \frac{\partial r V_r}{\partial r} \right) + \frac{1}{r^2} \frac{\partial^2 V_r}{\partial \theta^2} - \frac{2}{r^2} \frac{\partial V_\theta}{\partial \theta} + \frac{\partial^2 V_r}{\partial z^2} \right] \quad (2)$$

Z - direction

$$\rho \left[\frac{\partial V_z}{\partial t} + V_r \frac{\partial V_z}{\partial r} + \frac{V_\theta}{r} \frac{\partial V_z}{\partial \theta} + V_z \frac{\partial V_z}{\partial z} \right] = \rho g_z - \frac{dP}{dz} + \mu \left[\frac{1}{r} \frac{\partial}{\partial r} \left(r \frac{\partial V_z}{\partial r} \right) + \frac{1}{r^2} \frac{\partial^2 V_z}{\partial \theta^2} + \frac{\partial^2 V_z}{\partial z^2} \right] \quad (3)$$

Assuming an axially symmetric, rigid tube and thus negligible velocities in the R and θ directions, two classic solutions exist: Wormersley's solution to a non-zero pressure gradient and Poiseuille's solution to a zero pressure gradient. Wormersly's solution is presented first.

In its general form for a Newton fluid, the z direction equation reduces to

where,

- V_z = axial velocity
- μ = viscosity
- ρ = density
- P = pressure
- r = radius
- t = time
- ν = kinematic viscosity

Assume $\frac{dP}{dz}$ to be harmonic, such that

$$\frac{dP}{dz} = A * e^{i\omega t} \quad (4)$$

Substituting for $\frac{dP}{dz}$,

$$\frac{\partial^2 V_z}{\partial r^2} + \frac{1}{r} \frac{\partial V_z}{\partial r} - \frac{1}{v_z} \frac{\partial V_z}{\partial t} = -\frac{A^*}{\mu} e^{i\omega t} \quad (5)$$

Assuming $V_z = ue^{i\omega t}$,

$$\frac{\partial^2 u}{\partial r^2} + \frac{1}{r} \frac{\partial u}{\partial r} - \frac{i\omega}{v} u = -\frac{A^*}{\mu} \quad (6)$$

This is a form of Bessel's equation, and its solution requisite to the necessary boundary conditions, is

$$u = \frac{A^*}{i\omega\mu} \left[1 - \frac{J_0\left(r\left(\frac{\omega}{v}\right)^{\frac{1}{2}} i^{3/2}\right)}{J_0\left(R\left(\frac{\omega}{v}\right)^{\frac{1}{2}} i^{3/2}\right)} \right] \quad (7)$$

where $J_0(x i^{3/2})$ is a Bessel function of the first kind of order zero and complex argument. Its general form is

$$J_\nu = x^\nu \sum_{m=0}^{\infty} \frac{(-1)^m x^{2m}}{2^{2m+\nu} m! \Gamma(\nu+m+1)} \quad (8)$$

Using the substitution, $\alpha = R(\omega/v)^{\frac{1}{2}}$ (a number often tabulated) and $y = r/R$

$$V_z = \frac{A^* R^2}{i\omega\mu} \left[1 - \frac{J_0(\alpha y i^{3/2})}{J_0(\alpha i^{3/2})} \right] e^{i\omega t} \quad (9)$$

At this point the Bessel function may be represented in terms of a modulus and phase of its real part,

$$J_0(\alpha y i^{3/2}) = M_0(y) e^{i\theta(y)} \quad (10)$$

$$J_0(\alpha i^{3/2}) = M_0 e^{i\theta} \quad (11)$$

In the same fashion, the real part of $A^* e^{i\omega t}$ may be

written in terms of a modulus and phase,

$$A * e^{i\omega t} = M \cos(\omega t - \phi) \quad (12)$$

Using the substitutions, and that $\delta_o = \theta - \theta(y)$

$$V_z = \frac{M}{\omega \rho} \sin(\omega t - \phi) - \frac{M_o(y)}{M_o} \sin(\omega t - \phi - \delta_o) \quad (13)$$

Wormersly further reduced his equation by writing

$$h_o = \frac{M_o(y)}{M_o} \quad (14)$$

and introduced M'_o and ϵ_o by the following definition,

$$M_o = (1 + h_o^2 - 2h_o \cos \delta_o)^{\frac{1}{2}} \quad (15)$$

and,

$$\tan \epsilon_o = \frac{h_o \sin \delta_o}{1 - h_o \cos \delta_o} \quad (16)$$

such that

$$V_z = \frac{M}{\omega \rho} M'_o \sin(\omega t - \phi + \epsilon_o) \quad (17)$$

Since $\alpha^2 = R^2 \frac{\omega \rho}{\mu}$

$$V_z = \frac{MR^2 M'_o}{\mu \alpha^2} \sin(\omega t - \phi + \epsilon_o) \quad (\text{Wormersly}) \quad (18)$$

(see figure 1).

Poiseuille's model is considerably less complex. By making several assumptions, Poiseuille was able to reduce the Navier-Stokes equations to an integrable form. Poiseuille's assumptions were:

- (1) steady (time invariant) flow. This implies that all time dependent variables are zero.

$$\frac{d}{dt} = 0 \quad (19)$$

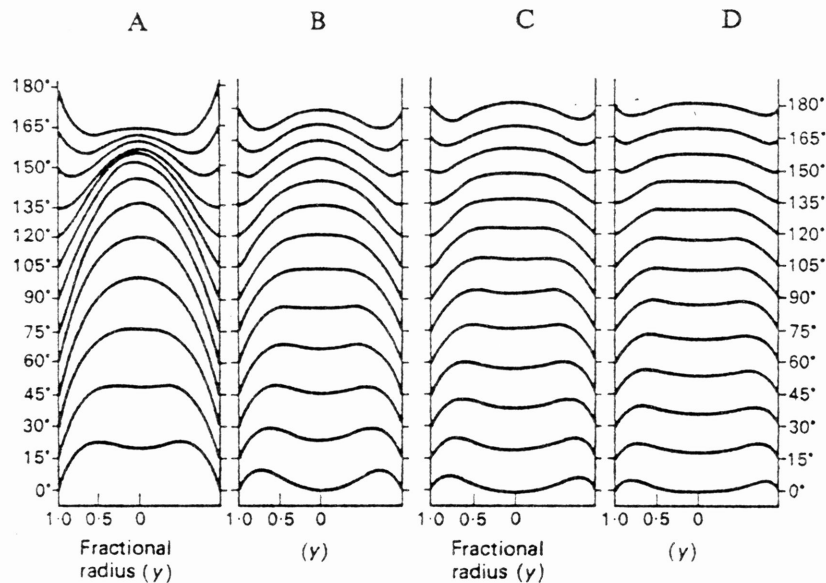


Fig. 5.1A. The velocity profiles, at intervals of 15° , of the flow resulting from a sinusoidal pressure-gradient ($\cos \omega t$) in a pipe. In this case, $\alpha = R \cdot \sqrt{\omega/\nu} = 3.34$, corresponding to the fundamental harmonic of the flow curves illustrated in Figs. 5.3 and 5.4. Note that reversal of flow starts in the laminae near the wall. As this is harmonic motion only half a cycle is illustrated as the remainder will be the same in form but opposite in sign, e.g. compare 180° and 0° .

B. A similar set of profiles for harmonic motion of double the frequency of A ($\alpha = 4.72$). The amplitude and phase of the pressure are the same here and in C and D as in A. The effects of the larger α are thus seen to be a flattening of the profile of the central region, a reduction of amplitude of the flow and the rate of reversal of flow increases close to the wall.

C. The third harmonic with $\alpha = 5.78$. The effects of higher frequency noted in B are here further accentuated.

D. The fourth harmonic ($\alpha = 6.67$) shows the same effects again. The rapidly varying part of the flow lies between $y = 0.8$ and $y = 1.0$ and the central mass of the fluid reciprocates almost like a solid core.

FIG. 1

(2) uniform flow profile. This assumption in combination with assumption 4 negates a radial and angular velocity. A uniform profile ensures that no turbulence exists within the system. Additionally, uniform flow assumes that the fluid undergoes no accelerations.

$$V_r = V_z = 0 \quad (20)$$

$$\frac{dV_z}{dz} = 0 \quad (21)$$

(3) the fluid is incompressible, homogenous and has a constant viscosity independent of the shear rate. This is the definition of a Newtonian fluid.

$$\rho = \text{constant}$$

$$\mu = \text{constant}$$

(4) rigid, circular pipe. At the wall of the tube, any change with respect to the radial direction must be zero.

$$\frac{d}{dr} = 0 \quad (22)$$

(5) symmetry. All functions dependent upon the theta direction are zero.

$$\frac{d}{d\theta} = 0 \quad (23)$$

(6) fully developed flow. That is, the region of study is distal to the entry region.

From the above assumptions, the Navier-Stokes equations can be reduced to the following:

R - direction

$$0 = \mu_r - \frac{dP}{dr} = \frac{dP'}{dr} \quad , \quad P' \neq f(r) \quad (24)$$

θ - direction

$$0 = g_0 - \frac{dP}{d\theta} = \frac{dP'}{d\theta} \quad (25)$$

z - direction

$$\frac{\mu}{r} \frac{d}{dr} \left(r \frac{dV_z}{dr} \right) = \frac{dP'}{dz} \quad (26)$$

The boundary conditions for this model are:

$$(1) \quad \left. \frac{dV_z}{dr} \right|_{r=0} = 0 \quad (27)$$

$$(2) \quad V_z \Big|_{r=R_0} = 0 \quad (28)$$

Solution of the above differential equation subjected to the boundary conditions will result in the Poiseuille model. Substituting $k = \frac{dP'}{dz}$ and solving,

$$\frac{rk}{\mu} = \frac{d}{dr} \left(r \frac{dV_z}{dr} \right) \quad (29)$$

Integrating,

$$C_1 + \frac{r^2 k}{2\mu} = r \frac{dV_z}{dr} \quad (30)$$

$$\left. \frac{dV_z}{dr} = 0 \right|_{r=0} \text{ yields } C_1 = 0.$$

$$\frac{rk}{2\mu} = \frac{dV_z}{dr} \quad (31)$$

Integrating,

$$C_2 + \frac{r^2 k}{4\mu} = V_z \quad (32)$$

For $r = R_o$,

$$0 = \frac{R_o^2}{4\mu} \frac{dP'}{dz} + C_2 \quad (33)$$

$$C_2 = - \frac{R_o^2}{4\mu} \frac{dP'}{dz} \quad (34)$$

Substituting,

$$V_z = \frac{R_o^2}{4\mu} \frac{dP'}{dz} \left[1 - \left(\frac{r}{R_o} \right)^2 \right] \quad (35)$$

From the resulting equation for axial velocity, it can be shown that the profile will be parabolic. The profile is dependent only upon r , as the pressure gradient was assumed to be constant.

To find the volume flow rate, Q , the velocity is integrated over the area.

$$Q = \int V_z \cdot dA \quad (36)$$

For cylindrical coordinates,

$$Q = \int_0^{2\pi} \int_0^{R_o} V_z r dr d\theta \quad (37)$$

$$Q = 2\pi \int_0^{R_o} r V_z dr \quad (38)$$

$$Q = 2\pi \int_0^{R_o} r \frac{1}{4\mu} \frac{dP'}{dz} (r^2 - R_o^2) \quad (39)$$

$$Q = \frac{2\pi}{4} \frac{dP'}{dz} \left(\frac{r^4}{4\mu} - \frac{R_o^2 r^2}{2\mu} \right) \Bigg|_0^{R_o} \quad (40)$$

ignoring the negative sign,

$$Q = \frac{\pi R_o^4}{8\mu} \frac{dP'}{dz} \quad (41)$$

McDonald drew the following conclusions as to the validity of applying Poiseuille's equation to blood flow.

(1) The fluid is homogenous and its viscosity is constant for all shear rates. Blood is a suspension of particles - notably red blood cells. If the dimensions of the vessel are large compared with the size of red blood cells, then blood can be considered a Newtonian fluid. The size restraint imposed by McDonald is an internal radius of 0.5 mm.

(2) The liquid does not slip at the wall. This was one of Poiseuille's boundary conditions - that is, $V_z=0$ at $r=R_o$. It has been shown that this condition is universally true for all fluids(1 ,5). One might project that presence of a plasma skimming layer might lead to slip. This point has never been proven experimentally.

(3) The flow is laminar. At lower flow rates, laminar flow is observed. If the flow rate exceeds a critical value, flow disturbances and turbulence in the fluid are seen. In some of the large arteries, turbulence is present. But for the smaller arteries and venous circulation, laminar flow is a fairly good assumption.

(4) The rate of fluid flow is 'steady' and is not subjected to any accelerations or decelerations. Since flow in the large arteries and the intrathoracic veins (2) is pulsatile, this assumption is not valid for that portion of the circulation.

(5) The tube is long compared with the region being studied. The transition region from a blunt velocity

profile to fully developed flow for a fluid is defined as its entry region. Within the entry region, the center portion of the flow is accelerated while the fluid near the wall is decelerated. Additionally, the pressure gradient in the entry region is not constant. Thus Poiseuille's law does not apply. (see figures 2 and 3)

(6) The tube is rigid; the diameter does not vary with the internal pressure. Blood vessels are distensible. Thus, the flow will not be completely determined by the pressure gradient.

A paper by Taylor and Gerrard (1977) closely parallels the intentions of this project for the non-stenosed case. Taylor and Gerrard presented a mathematical model utilizing the technique of finite differences to calculate the axial velocity as a function of time. The primary difference between their approach and the approach of this project is their inclusion of a skin friction term. This term takes into account viscous effects. It negates the importance of calculating the axial velocity as a function of the radius. Their results are presented in figure 4.

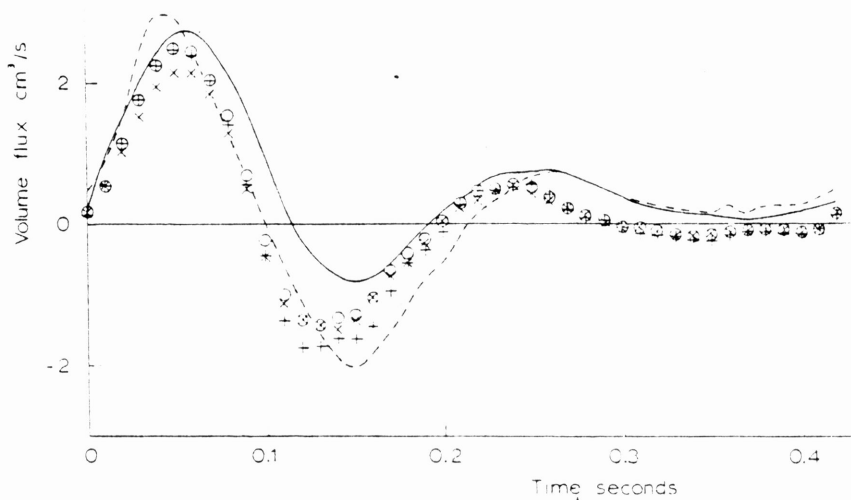


Fig. 1 Volume flux for one period of oscillation in a canine femoral artery
Streeter et al. (1963)

— experiment
- - - calculation

FIG. 4

Present model
+ skin friction = zero frequency value.
entrance-length correction included
× full linear treatment of the skin friction.
entrance-length correction included
.. as last without entrance-length correction

METHODS

An analytic solution to the general form of the Navier-Stokes equations would be extremely difficult.

A digital solution utilizing the technique of finite differences is more straight forward. Finite differences is a method for the approximation of a derivative. Central finite differences were chosen.

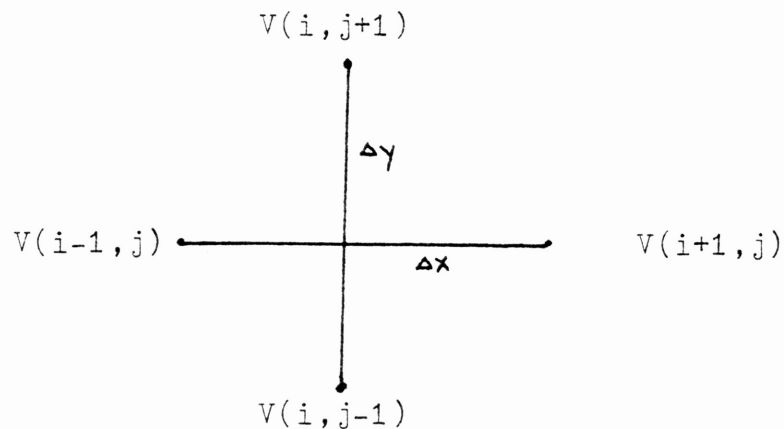
An approximation for the first derivative of a general function, Y, is:

$$\left. \frac{dY}{dx} \right|_{i,j} = \frac{Y(i+1,j) - Y(i-1,j)}{2\Delta x} \quad (42)$$

An approximation of the second derivative is:

$$\left. \frac{d^2Y}{dx^2} \right|_{i,j} = \frac{Y(i+1,j) + Y(i-1,j) - 2Y(i,j)}{\Delta x^2} \quad (43)$$

Recalling that symmetry was assumed, the following grid system can be used.



Similar grid systems can be chosen for approximations of $\frac{dP}{dz}$ and $\frac{dV}{dz}$.

Applying finite differences to the Navier-Stokes z-direction equation yields:

$$\begin{aligned}
& \rho \left[\frac{V_{i,j}^{n+1} - V_{i,j}^{n-1}}{2\Delta t} + V_{r,i,j}^n \left(\frac{V_{i,j+1}^n - V_{i,j-1}^n}{2\Delta r} \right) + V_{i,j}^n \left(\frac{V_{i,j+1}^n - V_{i,j-1}^n}{2\Delta z} \right) \right] \\
& = \rho g_z - \frac{P_{i,j+1}^n - P_{i,j-1}^n}{2\Delta z} + \mu \left[\frac{1}{r} \left(\frac{V_{i,j+1}^n - V_{i,j-1}^n}{2\Delta z} \right) + \right. \\
& \quad \left. \frac{V_{i+1,j}^n + V_{i-1,j}^n - 2V_{i,j}^n}{\Delta r^2} + \frac{V_{i,j+1}^n + V_{i,j-1}^n - 2V_{i,j}^n}{\Delta z^2} \right] \tag{44}
\end{aligned}$$

where,

- i = radial increment
- j = distal increment
- n = time increment
- t = time step size
- r = radial step size
- z = distal step size

solving for $V_{i,j}^{n+1}$ yields:

$$\begin{aligned}
V_{i,j}^{n+1} & = V_{i,j}^n + \frac{\Delta t}{\rho} \left[\rho g_z - \frac{\Delta P}{\Delta z} \right] + \frac{\Delta t}{\rho} \mu \left[\frac{1}{r} \left(\frac{V_{i,j+1}^n + V_{i,j-1}^n}{\Delta z} \right) \right. \\
& \quad \left. + \frac{V_{i+1,j}^n - 2V_{i,j}^n}{\Delta r^2} \right] + \frac{V_{i,j+2}^n + V_{i,j}^n - 2V_{i,j+1}^n}{\Delta z^2} \\
& \quad - \frac{\Delta t}{\rho} V_{i,j}^n \left[\frac{\Delta V_{i,j+1}^n - V_{i,j}^n}{\Delta z} \right] \tag{45}
\end{aligned}$$

An iterative solution to find V_z as a function of time is relatively simple. If $V_z(t=n)$ is known, then $V_z(t=n+1)$ can be found. The pressure gradient as a function of time can be approximated by obtaining two waveforms. At a particular time in the cycle, the

two pressures are subtracted and the difference is divided by the length between the points of measurement. All other parameters for this difference equation are known.

However, to start the iterative process, $V_z(t=0)$ at every point in the tube must be known. However, only the boundary conditions are known.

Within the coronary arteries, blood is rarely fully developed. Thus, the Poiseuille model can not be applied directly.

Viscous fluid theory in the entry region of rigid tube violates three of Poiseuille's assumptions:

(1) V_z is not a function of z . The principal difference between fully developed flow and entry region flow is that in the entry region, fluid elements experience accelerations - positive near the center of the tube, negative near the wall. Since the flow rate is a constant, no local acceleration exists. The acceleration of individual fluid elements is termed convective acceleration.

(2) The pressure gradient is a constant. The pressure gradient for a steady flow model falls linearly with distance only for Poiseuille flow. In the entry region there is a rapid non-linear pressure drop (see figure 5).

(3) Radial and/or angular velocities are zero. From the continuity equation (written for an incompressible fluid),

$$\frac{1}{r} \frac{\partial V_r}{\partial r} + \frac{1}{r} \frac{\partial V_\theta}{\partial \theta} + \frac{\partial V_z}{\partial z} = 0 \quad (46)$$

It can be demonstrated that both V_r and V_θ can not be zero. If so,

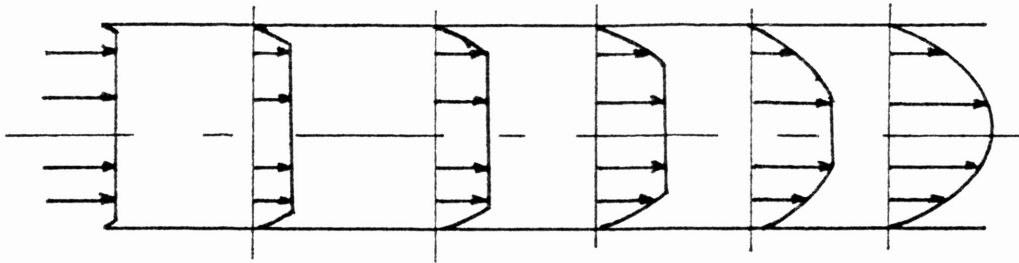


Fig. 2. The change in the velocity profile along the tube in steady flow indicating the growth of the boundary layer. The initially flat profile becomes modified to form the parabolic profile at a critical distance from the inlet.

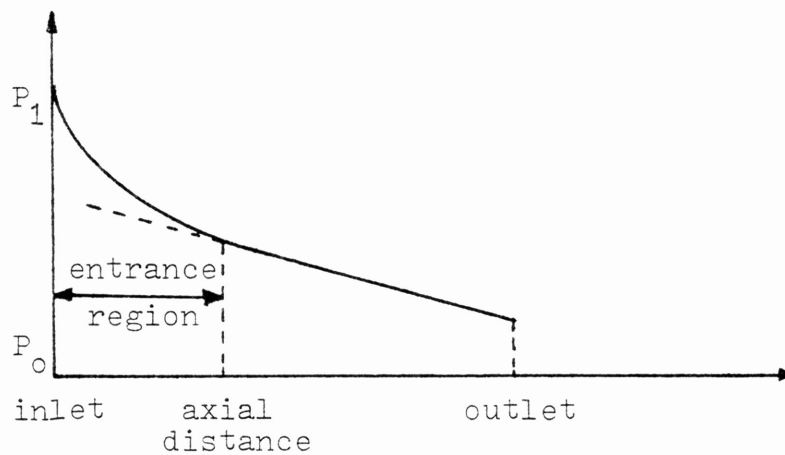


Fig. 3. The variation in local pressure as a function of distance from the inlet. In the entrance region the pressure falls rapidly with distance. Beyond the entry region, the pressure falls linearly with distance.

$$\frac{dV_z}{dz} = 0 \quad ; \quad V_z = \text{constant} \quad (47)$$

This is an obvious contradiction of condition 1.

If the remainder of Poiseuille's assumptions are kept and a radial velocity is assumed to exist rather than an angular velocity, the Navier-Stokes equations reduce to,

$$\rho \left[v_r \frac{\partial v_r}{\partial r} \right] = \rho g_r - \frac{dP}{dr} + \mu \left[\frac{\partial}{\partial r} \left(\frac{1}{r} \frac{\partial r v_r}{\partial r} \right) \right] \quad (48)$$

$$\rho \left[v_r \frac{\partial v_z}{\partial r} + v_z \frac{\partial v_z}{\partial z} \right] = \rho g_z - \frac{dP}{dz} + \mu \left[\frac{1}{r} \frac{\partial}{\partial r} \left(r \frac{\partial v_z}{\partial r} \right) + \frac{\partial^2 v_z}{\partial z^2} \right] \quad (49)$$

Solution of these coupled differential equations would prove difficult.

An important concept in viscous fluid theory is the development of the boundary layer. In the entry region fluid elements are sheared; the sheared elements become part of the boundary layer. The non-sheared elements comprise the free stream. As the fluid proceeds through the tube, a greater portion of its elements are sheared and thus its boundary layer grows. This is shown in figure 2.

The boundary layer thickness is defined as 99% of the radial distance from the vessel wall to the blunt portion of the profile. Obviously, the boundary layer thickness is a minimum for a totally blunt profile, and is a maximum for fully developed flow. The boundary layer thickness, δ , may be calculated from,

$$\delta = K \sqrt{\frac{\mu x}{\rho v}}$$

where, k = experimentally determined
proportionality constant
 x = distance from entrance

An important parameter of a fluid system is the Reynolds number. The Reynolds number is a dimensionless number representing the ratio of inertial to viscous forces. It is used as an indication to the state of a fluid. In general, laminar flow is observed for Reynolds numbers less than 2000. Turbulent flow is observed for Reynolds numbers greater than 3000. A transition region is seen for Reynolds numbers between 2000 and 3000. The Reynolds number, Re , can be calculated from:

$$Re = \frac{\rho U d}{\mu} \quad (51)$$

where d = diameter.

The inlet length defines the axial distance from the tube entrance at which the fluid first becomes fully developed. The inlet length, $XFULL$, can be calculated from:

$$XFULL = .03dRe \quad (52)$$

Poiseuille's solution to the Navier-Stokes equations is rather simple. Recall from equation 35 and 40 that the formulas to find axial velocity and flow rate are,

$$V_z = \frac{R_o^2}{4\mu} \frac{dP}{dz} \left[1 - \left(\frac{r}{R_o} \right)^2 \right] \quad (35)$$

$$Q = \frac{2\pi}{4\mu} \frac{dP}{dz} \left(\frac{R_o^2 r^2}{2} - \frac{r^4}{4} \right) \Bigg|_0^{R_o} \quad (40)$$

The mechanism for finding V_z and $\frac{dP}{dz}$ as functions of z is as follows:

(1) A value for δ , the boundary layer thickness is calculated from equation 50. The free stream velocity, U , from the profile of the previous distal increment was used, such that

$$\delta = K \sqrt{\frac{\mu x}{\rho U(x-1)}} \quad (53)$$

(2) Proceeding from the wall toward the tube center Poiseuille flow was assumed, and velocities were calculated from equation at particular radial increments. When the boundary layer thickness was reached, a final application of the equation was used.

(3) To find the free stream velocity the Poiseuille profile was integrated from the boundary layer thickness to the radius, RAD. This flow was termed QPAR. Assuming the volume flow rate, Q , to be constant, the free stream velocity can now be found from:

$$U = \frac{Q - QPAR}{(RAD - \delta)^2} \quad (54)$$

However, this method assumes a constant pressure gradient equal to the pressure of fully developed flow. This is clearly incorrect due to the discontinuity in the waveform (see figure 5).

A correct general shape for a velocity profile in entry region of a tube is shown in figure 6 (3).

A method of graphical correction of figure 5 to obtain figure 6 was used.

(4) The values of the slopes from point 1 to point 2 and from point 2 to point 3 are calculated. These are designated SLOPE1 (points 1 to 2), and SLOPE2 (points 2 to 3).

(5) Note in figure 6 that SLOPE1 is greater than SLOPE2. However, note also that SLOPE2 is not negative.

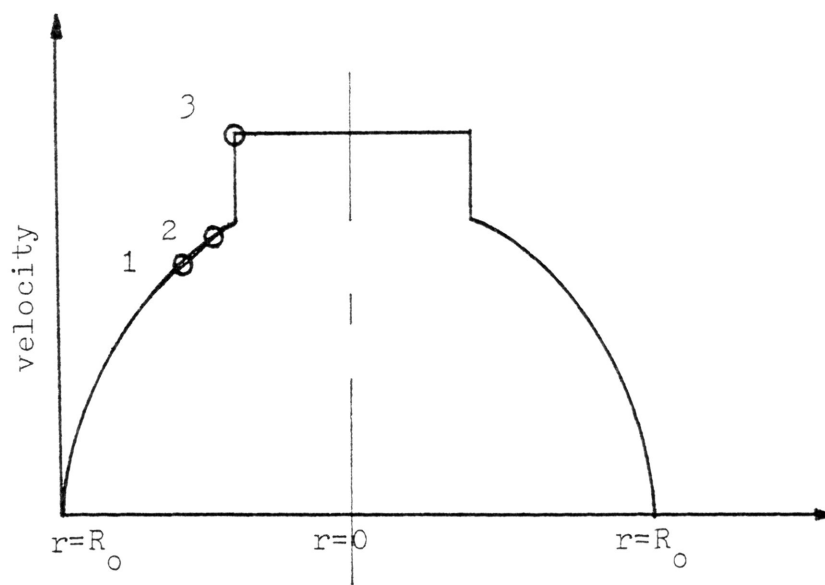


Fig. 5.

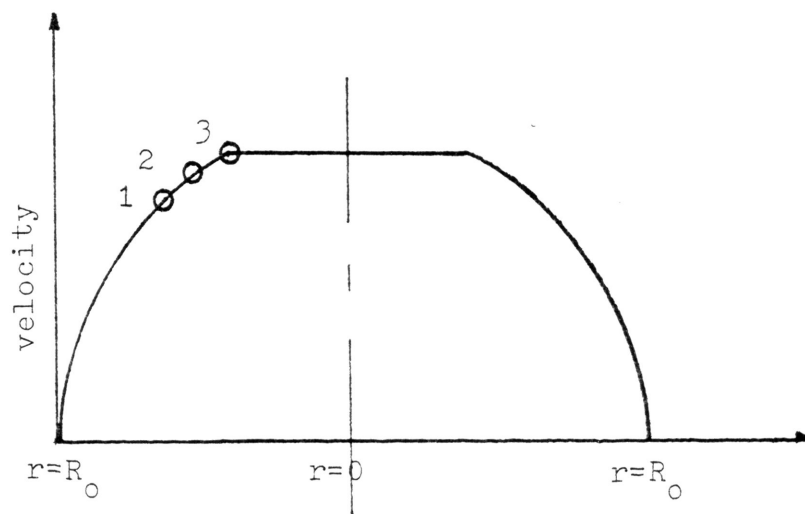


Fig 6.

In figure 5, SLOPE2 is obviously much greater than SLOPE1. By increasing the pressure gradient, a new velocity profile may be calculated. If once again, step 3 is applied, a new free stream velocity is found.

(6) SLOPE1 and SLOPE2 are recalculated. If SLOPE1 is still less than SLOPE2, the pressure gradient is incremented, and step 3 is repeated (followed by step 6). If SLOPE2 is negative, i.e., the free stream velocity is less than the velocity at the boundary layer thickness, the pressure gradient is decreased.

(7) The iterative process continues until SLOPE1 is greater than SLOPE2, and SLOPE2 is non-negative. The result is a value for $\frac{dP}{dz}$ which gives a continuous waveform.

A computer program was written using OS - WATFIV, the listing of which is located in appendix A. The program was run on the Amdahl 470V/6. The program used 15.11 seconds of CPU time. Computer plots of the output are listed in appendix B.

RESULTS AND CONCLUSIONS

Characteristics of the coronary arteries were found through out the literature. The following data were used. The volume flow rate was assumed to be 50 ml/min. The diameter of the left common coronary was assumed to be 3 mm.

Blood was assumed to have a density of 1.05g/cc and a viscosity of 3.0cp.

The pressure for fully developed flow was calculated by knowing the flow rate. The pressure gradient allowed calculation of the velocity profile for Poiseuille flow. The free stream velocity was found to be 23.576 cm/sec.

The Reynolds number was calculated to be 123.80.

The inlet length equaled 1.114 cm.

Realizing the free stream velocity for fully developed flow, the inlet length and that the boundary layer thickness for Poiseuille flow equals the radius, the proportionality constant, CST, was calculated. CST was found to be 4.042.

The results obtained are consistent with theory and with the literature.

In fact, the pressure gradient dropped rapidly in the entry region (see figure 7, table 1). The gradient eventually leveled at the fully developed value of 125.75 dynes/cc.

If additional computer money had been available, the more interesting region of the tube (the initial .07 cm) could have been investigated more rigorously. A significant step down in distal increment size may have shown a pressure gradient greater than the value of 183.33 dynes/cc listed. An attempt at a 100 increment code rather than the 40 increment code used was made. But execution time exceeded 40 seconds. Although this is not an immense job, funds were limited.

Appendix B shows computer plots of velocity profiles taken once every 4 distal increments. The profiles demonstrate that the process of graphical correction did, in fact, work. The profile developed quite rapidly. This was the most surprising portion of the program. Apparently, blood flow is considerably more dependent upon viscous effects than on its inertial effects.

At certain points, identical profiles were obtained for different values of the boundary layer thickness. This error is easily explained. Due to the magnitude of the radial step size, it was possible for two (or more) values of the boundary thickness to share a radial point as a cut-off for the Poisuille profile.

TABLE 1

<u>INLET LENGTH</u>	<u>BOUNDARY LAYER THICKNESS</u>	<u>PRESSURE GRADIENT</u>
0.02717	0.032798	183.33
0.05434	0.041033	165.06
0.08151	0.049064	148.16
0.10869	0.054724	144.21
0.13586	0.060493	138.28
0.16304	0.064858	135.95
0.19021	0.069320	134.06
0.21738	0.073372	132.23
0.24456	0.077015	131.01
0.27173	0.080424	129.97
0.29890	0.083623	129.06
0.32607	0.086594	128.29
0.35325	0.089369	128.29
0.38042	0.092743	127.65
0.40759	0.095210	127.14
0.43477	0.097569	126.76
0.46194	0.099868	126.76
0.48911	0.10276	126.51
0.51628	0.10498	126.51
0.54346	0.10770	126.26
0.57063	0.10964	126.13
0.59780	0.11174	126.13
0.62497	0.11426	126.00
0.65215	0.11615	126.00
0.67932	0.11854	125.88
0.70649	0.12016	125.82
0.73367	0.12192	125.82
0.76084	0.12416	125.82
0.78801	0.12628	125.82
0.81518	0.12844	125.76
0.84236	0.12969	125.76
0.86953	0.13177	125.75

<u>INLET LENGTH</u>	<u>BOUNDARY LAYER THICKNESS</u>	<u>PRESSURE GRADIENT</u>
0.89670	0.13356	125.75
0.92388	0.13557	125.75
0.95105	0.13740	125.75
0.97822	0.13935	125.75
1.0054	0.14116	125.75
1.0326	0.14305	125.75
1.0597	0.14485	125.75
1.0869	0.14670	125.75

PRESSURE GRADIENT IN THE ENTRY REGION

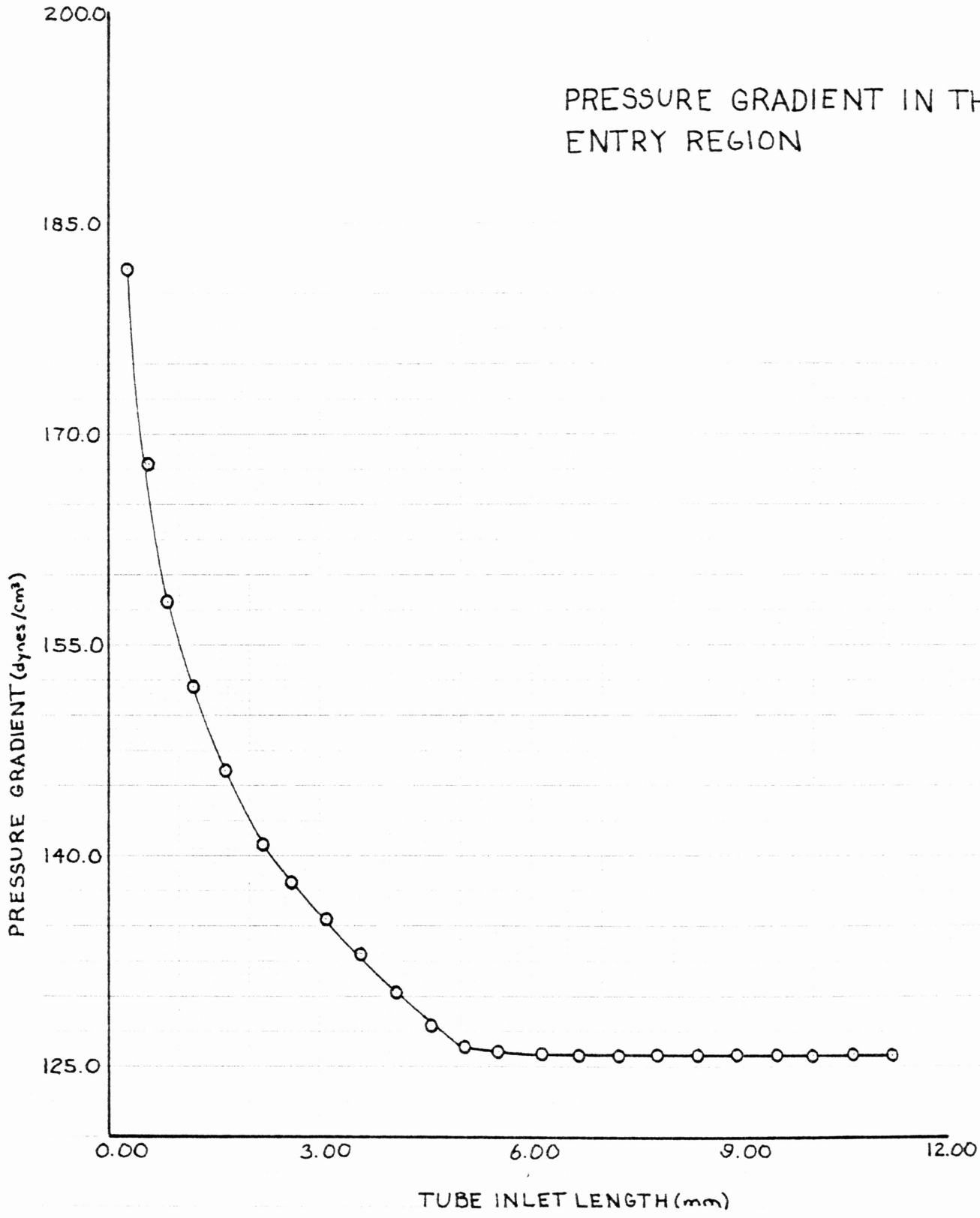


FIG. 7

This necessarily forced an identical profile and thus an identical pressure gradient. A simple solution to this error would be to reduce the radial step size.

REFERENCES

1. Birchoff, G.(1960). Hydrodynamics. Princeton University Press.
2. Brecher, G.A.(1956). Venous Return. New York; Grune and Stratton.
3. Caro, C.G., Pedley, T.J., Schroeter,R.C., and Seed, W.A. The Mechanics of the Circulation. New York: Oxford University Press, 1978, pp.44-55.
4. Guyton, A.C., M.D. Medical Physiology. Philadelphia W.B. Saunders Company, 1976, pp.324-330.
5. Kaufmann, W.(1963). Fluid Mechanics. translated by E.C.Chilton. New York: McGraw Hill.
6. McDonald, D.A.,Blood Flow in Arteries. Baltimore: Williams and Wilkins Company, 1974, pp.27-30.
7. May, A.G., DeWeese, J.A., and Rob, C.G.: Hemodynamics effects of arterial stenosis. Surgery, 53:513,1963.
8. Smith, R.L., Blick, E.F., Coalson, J. and Stein, P.D.: Thrombus production by turbulence. J Appl Physiol, 32:261, 1972
9. Stehbens, W.E., editor. Hemodynamics and the Blood Vessel Wall. Springfield, Ill.: Charles C. Thomas, 1979, pp.447-455.
10. Taylor, L.A., and Gerrard, J.H.: Mathematical model representing blood flow in arteries. Med & Biol Eng. & Comput, 15:611-617, 1977.
11. Webster, John G., editor. Medical Instrumentation: Application and Design. Boston: Houghton Mifflin Company, 1978, pp.409-412.
12. Wormersley, J.R.(1955b). Method for the calculation of velocity, rate of flow and viscous drag in arteries when the pressure gradient is known J Appl Physiol.,127:553-563.

Appendix A
Computer Code Listing

7/EDITIONS

LITH IST

A COMPUTER CODE HAS BEEN WRITTEN WHICH CALCULATES THE
VELOCITY PROFILE AND PRESSURE GRADIENT IN A RIGID TUBE
AS A FUNCTION OF THE TUBE LENGTH. THE METHOD BY WHICH
THIS WAS ACCOMPLISHED IS DESCRIBED IN THE TEXT.

TABLE OF VARIABLES

CST - PROPORTIONALITY CONSTANT RELATING THE BOUNDARY LAYER
THICKNESS TO THE FREE STREAM VELOCITY AND THE INLET
LENGTH.

DELMAX - EQUAL TO THE RADIUS AND USED TO CALCULATE THE TRACT
LENGTH. IT REPRESENTS THE MAXIMUM BOUNDARY LAYER
THICKNESS.

DELTA - THE BOUNDARY THICKNESS

DIAM - TUBE DIAMETER

DIRINC - THE DISTAL INCREMENT

DPDZ - THE PRESSURE GRADIENT WITH RESPECT TO THE AXIAL
DIRECTION.

FRVEL - THE ENTERING FREE STREAM VELOCITY. IT IS FOUND
BY DIVIDING THE VOLUME FLOW RATE BY THE AREA.

INIT - SUBROUTINE WHICH CALCULATES THE VELOCITY PROFILE

AND SUBSEQUENTLY THE PRESSURE GRADIENT.

MU - BLOOD VISCOSITY

NO - SEE COMMENTED SUBROUTINE PLOTLP

NPLOTS - SEE COMMENTED SUBROUTINE PLOTLP

NPTS - SEE COMMENTED SUBROUTINE PLOTLP
WHICH PLOTS THE VELOCITY AS A FUNCTION
OF THE RADIUS.

Q - VOLUME FLOW RATE.

QA - USED TO CALCULATE THE POISEUILLE FLOW RATE QUP TO VISCOUS


```

8
9
10
11
12
13
14
15
16
17
18
19
20
21
22
23
24
25
26
27
28
29
30
31
32
33
34
35
36
37
38
39
40
41
42
43
44
45
46
47
48
49
50
51
52
53
54
55
56
57
58
59
60
61
62
63
64
65
66
67
68
69
70
71
72
73
74
75
76
77
78
79
80
81
82
83
84
85
86
87
88
89
90
91
92
93
94
95
96
97
98
99
100
101
102
103
104
105
106
107
108
109
110
111
112
113
114
115
116
117
118
119
120
121
122
123
124
125
126
127
128
129
130
131
132
133
134
135
136
137
138
139
140
141
142
143
144
145
146
147
148
149
150
151
152
153
154
155
156
157
158
159
160
161
162
163
164
165
166
167
168
169
170
171
172
173
174
175
176
177
178
179
180
181
182
183
184
185
186
187
188
189
190
191
192
193
194
195
196
197
198
199
200
201
202
203
204
205
206
207
208
209
210
211
212
213
214
215
216
217
218
219
220
221
222
223
224
225
226
227
228
229
230
231
232
233
234
235
236
237
238
239
240
241
242
243
244
245
246
247
248
249
250
251
252
253
254
255
256
257
258
259
260
261
262
263
264
265
266
267
268
269
270
271
272
273
274
275
276
277
278
279
280
281
282
283
284
285
286
287
288
289
290
291
292
293
294
295
296
297
298
299
300
301
302
303
304
305
306
307
308
309
310
311
312
313
314
315
316
317
318
319
320
321
322
323
324
325
326
327
328
329
330
331
332
333
334
335
336
337
338
339
340
341
342
343
344
345
346
347
348
349
350
351
352
353
354
355
356
357
358
359
360
361
362
363
364
365
366
367
368
369
370
371
372
373
374
375
376
377
378
379
380
381
382
383
384
385
386
387
388
389
390
391
392
393
394
395
396
397
398
399
400
401
402
403
404
405
406
407
408
409
410
411
412
413
414
415
416
417
418
419
420
421
422
423
424
425
426
427
428
429
430
431
432
433
434
435
436
437
438
439
440
441
442
443
444
445
446
447
448
449
450
451
452
453
454
455
456
457
458
459
460
461
462
463
464
465
466
467
468
469
470
471
472
473
474
475
476
477
478
479
480
481
482
483
484
485
486
487
488
489
490
491
492
493
494
495
496
497
498
499
500
501
502
503
504
505
506
507
508
509
510
511
512
513
514
515
516
517
518
519
520
521
522
523
524
525
526
527
528
529
530
531
532
533
534
535
536
537
538
539
540
541
542
543
544
545
546
547
548
549
550
551
552
553
554
555
556
557
558
559
560
561
562
563
564
565
566
567
568
569
570
571
572
573
574
575
576
577
578
579
580
581
582
583
584
585
586
587
588
589
590
591
592
593
594
595
596
597
598
599
600
601
602
603
604
605
606
607
608
609
610
611
612
613
614
615
616
617
618
619
620
621
622
623
624
625
626
627
628
629
630
631
632
633
634
635
636
637
638
639
640
641
642
643
644
645
646
647
648
649
650
651
652
653
654
655
656
657
658
659
660
661
662
663
664
665
666
667
668
669
670
671
672
673
674
675
676
677
678
679
680
681
682
683
684
685
686
687
688
689
690
691
692
693
694
695
696
697
698
699
700
701
702
703
704
705
706
707
708
709
710
711
712
713
714
715
716
717
718
719
720
721
722
723
724
725
726
727
728
729
730
731
732
733
734
735
736
737
738
739
740
741
742
743
744
745
746
747
748
749
750
751
752
753
754
755
756
757
758
759
760
761
762
763
764
765
766
767
768
769
770
771
772
773
774
775
776
777
778
779
780
781
782
783
784
785
786
787
788
789
790
791
792
793
794
795
796
797
798
799
800
801
802
803
804
805
806
807
808
809
810
811
812
813
814
815
816
817
818
819
820
821
822
823
824
825
826
827
828
829
830
831
832
833
834
835
836
837
838
839
840
841
842
843
844
845
846
847
848
849
850
851
852
853
854
855
856
857
858
859
860
861
862
863
864
865
866
867
868
869
870
871
872
873
874
875
876
877
878
879
880
881
882
883
884
885
886
887
888
889
890
891
892
893
894
895
896
897
898
899
900
901
902
903
904
905
906
907
908
909
910
911
912
913
914
915
916
917
918
919
920
921
922
923
924
925
926
927
928
929
930
931
932
933
934
935
936
937
938
939
940
941
942
943
944
945
946
947
948
949
950
951
952
953
954
955
956
957
958
959
960
961
962
963
964
965
966
967
968
969
970
971
972
973
974
975
976
977
978
979
980
981
982
983
984
985
986
987
988
989
990
991
992
993
994
995
996
997
998
999
1000

```

```

39      DO 30 JJ=2,11
40      XX=(JJ-1)*DHICP
41      DELTA=CST*(MU**XX)/(VEL(41,JJ-1,1)*RHC))**5
42      WRITE(6,600)X,DLTA
43      FORMAT(1,'//////////120,FRG-A-TUBR-INLET-LENGTH-DE',
44      * 012.5,2X,'THE BOUNDARY LAYER THICKNESS, DELTA 5,012.5,2X,
45      *CM,//////)
46      FORMAT(1,'//1233,INLET LENGTH (C1),ATCS,RADIAL DISTANCE (
47      *CM),T98,VELOCITY (CM/SEC),//)
48      STORE=DDZ
49      C POISEUILLE'S MODEL IS USED TO CALCULATE THE VELOCITY AS A
50      C FUNCTION OF THE RADIUS.
51      C
52      C
53      DO 60 LL=1,500
54      DO 70 JJ=1,41
55      L=41-JJ
56      REL=RNCR
57      VEL(JJ,JJ,1)=RAD**2*DPDZ*(1-(R/RAD)**2)/(4*MU)
58      IF(II*GE,41)GOTO88
59      C AN IF STATEMENT IS USED TO DETERMINE IF THE BLUNT PROFILE HAS
60      C BEEN REACHED YET.
61      C
62      C
63      IF(2*LF,RAD-DELTA)GOTO 22
64      C 40 CONTINUE
65      C
66      C THE VELOCITY IS INTEGRATED OVER THE AREA TO FIND THE VOLUME
67      C FLOW RATE.
68      C
69      DO 20 00=PI*DDZ*(2.00*MU)*(RAD**4/2*(C0-RAD**2/4)*D0)
70      0A=PI*DDZ*(2.00*MU)*(RAD**2*(R**2/2.00-R**4/4)*D0)
71      0B=R*00-0A
72      VEL=CVEL(11,1,JJ,1)=(C-0A*0B)/(01*0B**2)
73      *EXTENSION* OTHER COMPUTERS MAY NOT ALLOW MULTIPLE ASSIGNMENT STATEMENTS
74      IF(11*GE,40)GOTO88
75      K=11+2
76      DO 50 K=1K,41
77      2=0-RNCR
78      VEL(K,JJ,1)=VELUC
79      C 50 CONTINUE
80      C
81      C THE SLOPES AROUND THE TRANSITION TO THE BLUNT PROFILE ARE
82      C FOUND. THESE ARE USED TO FIT THE PROFILE TO A CONTINUOUS
83      C WAVEFORM.
84      C
85      SL1=(VEL(11,JJ,1)-VEL(11-1,JJ,1))/RNCR
86      SL2=(VEL(11,1,JJ,1)-VEL(11,JJ,1))/RNCR
87      IF(SL2-CT,0)GOTO44
88      IF(SL1*G1,SL2)GOTO88
89      00DZ=1.01*DFDZ
90      44 00DZ=DDZ/1.0015005
91      88 00DZ=0
92      88 0=PAD
93      WRITE(6,700)
94      FORMAT(1,'//150,DEZ =,C14*5,2X,CVMP5/CUBIC CM',
95      * 00 70 ME=1,41

```

184
 185
 186
 187
 188
 189
 190
 191
 192
 193
 194
 195
 196
 197
 198
 199
 200
 201
 202
 203
 204
 205
 206
 207
 208
 209
 210
 211
 212
 213
 214
 215
 216
 217
 218
 219
 220
 221
 222
 223
 224
 225
 226
 227
 228
 229
 230
 231
 232
 233
 234
 235
 236
 237
 238
 239
 240
 241


```

00004500
00005000
00005100
00005200
00005300
00005400
00005500
00005600
00005700
00005800
00005900
00006000
00006100
00006200
00006300
00006400
00006500
00006600
00006700
00006800
00006900
00007000
00007100
00007200
00007300
00007400
00007500
00007600
00007700
00007800
00007900
00008000
00008100
00008200
00008300
00008400
00008500
00008600
00008700
00008800
00008900
00009000
00009100
00009200
00009300
00009400
00009500
00009600
00009700
00009800
00009900

```

```

C THE CURVES ARE IDENTIFIED BY THE PRINT CHARACTERS USED, WHICH
C ARE THE NUMBERS 1 THRU 9. SHOULD TWO OR MORE CURVES HAVE
C VALUES WHICH OCCUPY THE SAME PRINT POSITION, THE LARGEST
C NUMERIC CHARACTER IS PRINTED.
C
C NO PAGE EJECT IS MADE PRIOR TO PRINTING. SO USER MUST PROVIDE
C LINE IF HE DESIRES TO HAVE PLOT ON 'CLEAN' SHEET OF PAPER.

```

```

C REFERENCE
C ADAPTED FROM UT - ARLINGTON PLOT PACKAGE BY P. R. WIER
C TAMU COMPUTER SCIENCE DEPARTMENT - 10 APRIL, 1978

```

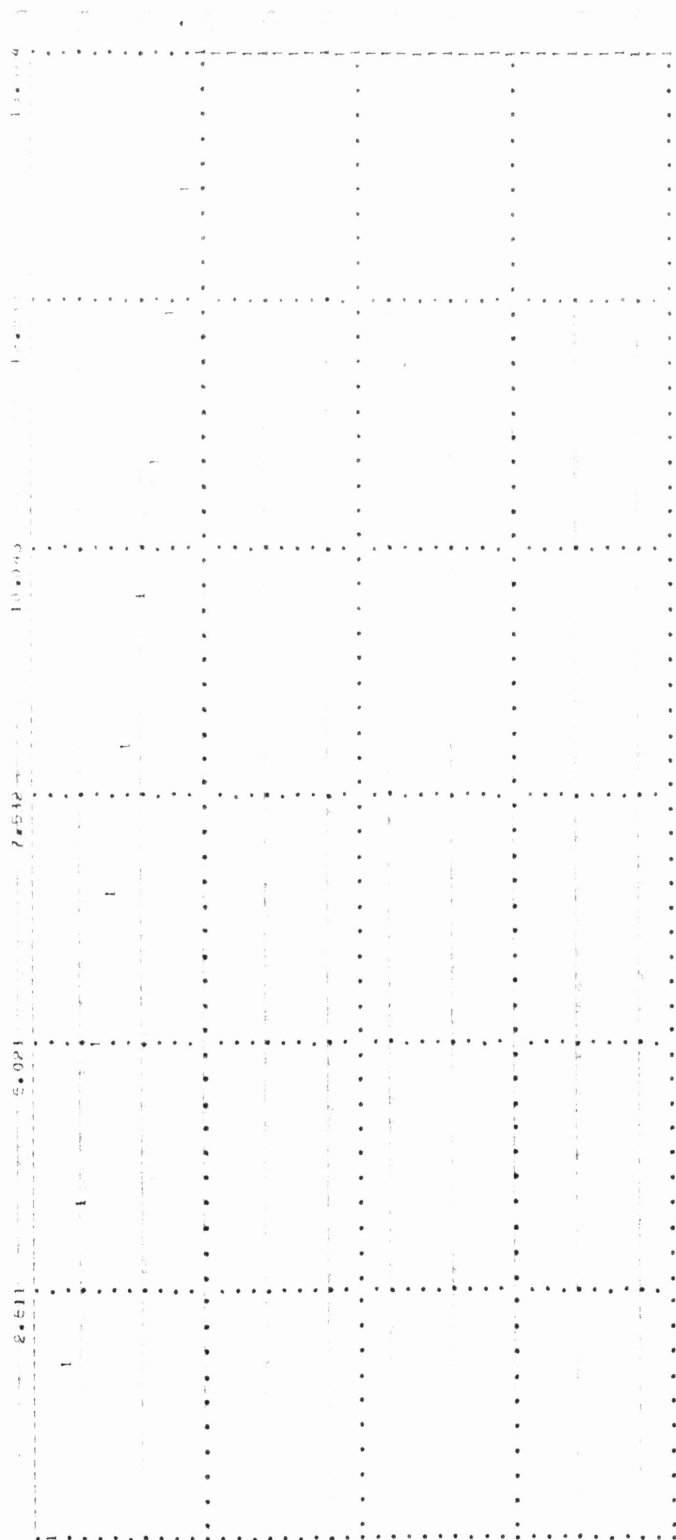
```

87 SUBROUTINE PLOT (XSTART, XINC, Y, NPLOTS, NPTS, ND, DIMENSION Y(ND, NPTS),
C *D, LINE(1), MARK(1:2)), (X1, X2, Y1, Y2), (X3, X4, Y3, Y4), (X5, X6, Y5, Y6),
C *S1, S2, S3, S4, S5, S6, S7, S8, S9, S10, S11, S12, S13, S14, S15, S16, S17, S18, S19, S20,
C *DASH, *DASH2, *DASH3, *DASH4, *DASH5, *DASH6, *DASH7, *DASH8, *DASH9, *DASH10,
C *DASH11, *DASH12, *DASH13, *DASH14, *DASH15, *DASH16, *DASH17, *DASH18, *DASH19, *DASH20,
C *DASH21, *DASH22, *DASH23, *DASH24, *DASH25, *DASH26, *DASH27, *DASH28, *DASH29, *DASH30,
C *DASH31, *DASH32, *DASH33, *DASH34, *DASH35, *DASH36, *DASH37, *DASH38, *DASH39, *DASH40,
C *DASH41, *DASH42, *DASH43, *DASH44, *DASH45, *DASH46, *DASH47, *DASH48, *DASH49, *DASH50,
C *DASH51, *DASH52, *DASH53, *DASH54, *DASH55, *DASH56, *DASH57, *DASH58, *DASH59, *DASH60,
C *DASH61, *DASH62, *DASH63, *DASH64, *DASH65, *DASH66, *DASH67, *DASH68, *DASH69, *DASH70,
C *DASH71, *DASH72, *DASH73, *DASH74, *DASH75, *DASH76, *DASH77, *DASH78, *DASH79, *DASH80,
C *DASH81, *DASH82, *DASH83, *DASH84, *DASH85, *DASH86, *DASH87, *DASH88, *DASH89, *DASH90,
C *DASH91, *DASH92, *DASH93, *DASH94, *DASH95, *DASH96, *DASH97, *DASH98, *DASH99, *DASH100,
C *DASH101, *DASH102, *DASH103, *DASH104, *DASH105, *DASH106, *DASH107, *DASH108, *DASH109, *DASH110,
C *DASH111, *DASH112, *DASH113, *DASH114, *DASH115, *DASH116, *DASH117, *DASH118, *DASH119, *DASH120,
C *DASH121, *DASH122, *DASH123, *DASH124, *DASH125, *DASH126, *DASH127, *DASH128, *DASH129, *DASH130,
C *DASH131, *DASH132, *DASH133, *DASH134, *DASH135, *DASH136, *DASH137, *DASH138, *DASH139, *DASH140,
C *DASH141, *DASH142, *DASH143, *DASH144, *DASH145, *DASH146, *DASH147, *DASH148, *DASH149, *DASH150,
C *DASH151, *DASH152, *DASH153, *DASH154, *DASH155, *DASH156, *DASH157, *DASH158, *DASH159, *DASH160,
C *DASH161, *DASH162, *DASH163, *DASH164, *DASH165, *DASH166, *DASH167, *DASH168, *DASH169, *DASH170,
C *DASH171, *DASH172, *DASH173, *DASH174, *DASH175, *DASH176, *DASH177, *DASH178, *DASH179, *DASH180,
C *DASH181, *DASH182, *DASH183, *DASH184, *DASH185, *DASH186, *DASH187, *DASH188, *DASH189, *DASH190,
C *DASH191, *DASH192, *DASH193, *DASH194, *DASH195, *DASH196, *DASH197, *DASH198, *DASH199, *DASH200,
C *DASH201, *DASH202, *DASH203, *DASH204, *DASH205, *DASH206, *DASH207, *DASH208, *DASH209, *DASH210,
C *DASH211, *DASH212, *DASH213, *DASH214, *DASH215, *DASH216, *DASH217, *DASH218, *DASH219, *DASH220,
C *DASH221, *DASH222, *DASH223, *DASH224, *DASH225, *DASH226, *DASH227, *DASH228, *DASH229, *DASH230,
C *DASH231, *DASH232, *DASH233, *DASH234, *DASH235, *DASH236, *DASH237, *DASH238, *DASH239, *DASH240,
C *DASH241, *DASH242, *DASH243, *DASH244, *DASH245, *DASH246, *DASH247, *DASH248, *DASH249, *DASH250,
C *DASH251, *DASH252, *DASH253, *DASH254, *DASH255, *DASH256, *DASH257, *DASH258, *DASH259, *DASH260,
C *DASH261, *DASH262, *DASH263, *DASH264, *DASH265, *DASH266, *DASH267, *DASH268, *DASH269, *DASH270,
C *DASH271, *DASH272, *DASH273, *DASH274, *DASH275, *DASH276, *DASH277, *DASH278, *DASH279, *DASH280,
C *DASH281, *DASH282, *DASH283, *DASH284, *DASH285, *DASH286, *DASH287, *DASH288, *DASH289, *DASH290,
C *DASH291, *DASH292, *DASH293, *DASH294, *DASH295, *DASH296, *DASH297, *DASH298, *DASH299, *DASH300,
C *DASH301, *DASH302, *DASH303, *DASH304, *DASH305, *DASH306, *DASH307, *DASH308, *DASH309, *DASH310,
C *DASH311, *DASH312, *DASH313, *DASH314, *DASH315, *DASH316, *DASH317, *DASH318, *DASH319, *DASH320,
C *DASH321, *DASH322, *DASH323, *DASH324, *DASH325, *DASH326, *DASH327, *DASH328, *DASH329, *DASH330,
C *DASH331, *DASH332, *DASH333, *DASH334, *DASH335, *DASH336, *DASH337, *DASH338, *DASH339, *DASH340,
C *DASH341, *DASH342, *DASH343, *DASH344, *DASH345, *DASH346, *DASH347, *DASH348, *DASH349, *DASH350,
C *DASH351, *DASH352, *DASH353, *DASH354, *DASH355, *DASH356, *DASH357, *DASH358, *DASH359, *DASH360,
C *DASH361, *DASH362, *DASH363, *DASH364, *DASH365, *DASH366, *DASH367, *DASH368, *DASH369, *DASH370,
C *DASH371, *DASH372, *DASH373, *DASH374, *DASH375, *DASH376, *DASH377, *DASH378, *DASH379, *DASH380,
C *DASH381, *DASH382, *DASH383, *DASH384, *DASH385, *DASH386, *DASH387, *DASH388, *DASH389, *DASH390,
C *DASH391, *DASH392, *DASH393, *DASH394, *DASH395, *DASH396, *DASH397, *DASH398, *DASH399, *DASH400,
C *DASH401, *DASH402, *DASH403, *DASH404, *DASH405, *DASH406, *DASH407, *DASH408, *DASH409, *DASH410,
C *DASH411, *DASH412, *DASH413, *DASH414, *DASH415, *DASH416, *DASH417, *DASH418, *DASH419, *DASH420,
C *DASH421, *DASH422, *DASH423, *DASH424, *DASH425, *DASH426, *DASH427, *DASH428, *DASH429, *DASH430,
C *DASH431, *DASH432, *DASH433, *DASH434, *DASH435, *DASH436, *DASH437, *DASH438, *DASH439, *DASH440,
C *DASH441, *DASH442, *DASH443, *DASH444, *DASH445, *DASH446, *DASH447, *DASH448, *DASH449, *DASH450,
C *DASH451, *DASH452, *DASH453, *DASH454, *DASH455, *DASH456, *DASH457, *DASH458, *DASH459, *DASH460,
C *DASH461, *DASH462, *DASH463, *DASH464, *DASH465, *DASH466, *DASH467, *DASH468, *DASH469, *DASH470,
C *DASH471, *DASH472, *DASH473, *DASH474, *DASH475, *DASH476, *DASH477, *DASH478, *DASH479, *DASH480,
C *DASH481, *DASH482, *DASH483, *DASH484, *DASH485, *DASH486, *DASH487, *DASH488, *DASH489, *DASH490,
C *DASH491, *DASH492, *DASH493, *DASH494, *DASH495, *DASH496, *DASH497, *DASH498, *DASH499, *DASH500,
C *DASH501, *DASH502, *DASH503, *DASH504, *DASH505, *DASH506, *DASH507, *DASH508, *DASH509, *DASH510,
C *DASH511, *DASH512, *DASH513, *DASH514, *DASH515, *DASH516, *DASH517, *DASH518, *DASH519, *DASH520,
C *DASH521, *DASH522, *DASH523, *DASH524, *DASH525, *DASH526, *DASH527, *DASH528, *DASH529, *DASH530,
C *DASH531, *DASH532, *DASH533, *DASH534, *DASH535, *DASH536, *DASH537, *DASH538, *DASH539, *DASH540,
C *DASH541, *DASH542, *DASH543, *DASH544, *DASH545, *DASH546, *DASH547, *DASH548, *DASH549, *DASH550,
C *DASH551, *DASH552, *DASH553, *DASH554, *DASH555, *DASH556, *DASH557, *DASH558, *DASH559, *DASH560,
C *DASH561, *DASH562, *DASH563, *DASH564, *DASH565, *DASH566, *DASH567, *DASH568, *DASH569, *DASH570,
C *DASH571, *DASH572, *DASH573, *DASH574, *DASH575, *DASH576, *DASH577, *DASH578, *DASH579, *DASH580,
C *DASH581, *DASH582, *DASH583, *DASH584, *DASH585, *DASH586, *DASH587, *DASH588, *DASH589, *DASH590,
C *DASH591, *DASH592, *DASH593, *DASH594, *DASH595, *DASH596, *DASH597, *DASH598, *DASH599, *DASH600,
C *DASH601, *DASH602, *DASH603, *DASH604, *DASH605, *DASH606, *DASH607, *DASH608, *DASH609, *DASH610,
C *DASH611, *DASH612, *DASH613, *DASH614, *DASH615, *DASH616, *DASH617, *DASH618, *DASH619, *DASH620,
C *DASH621, *DASH622, *DASH623, *DASH624, *DASH625, *DASH626, *DASH627, *DASH628, *DASH629, *DASH630,
C *DASH631, *DASH632, *DASH633, *DASH634, *DASH635, *DASH636, *DASH637, *DASH638, *DASH639, *DASH640,
C *DASH641, *DASH642, *DASH643, *DASH644, *DASH645, *DASH646, *DASH647, *DASH648, *DASH649, *DASH650,
C *DASH651, *DASH652, *DASH653, *DASH654, *DASH655, *DASH656, *DASH657, *DASH658, *DASH659, *DASH660,
C *DASH661, *DASH662, *DASH663, *DASH664, *DASH665, *DASH666, *DASH667, *DASH668, *DASH669, *DASH670,
C *DASH671, *DASH672, *DASH673, *DASH674, *DASH675, *DASH676, *DASH677, *DASH678, *DASH679, *DASH680,
C *DASH681, *DASH682, *DASH683, *DASH684, *DASH685, *DASH686, *DASH687, *DASH688, *DASH689, *DASH690,
C *DASH691, *DASH692, *DASH693, *DASH694, *DASH695, *DASH696, *DASH697, *DASH698, *DASH699, *DASH700,
C *DASH701, *DASH702, *DASH703, *DASH704, *DASH705, *DASH706, *DASH707, *DASH708, *DASH709, *DASH710,
C *DASH711, *DASH712, *DASH713, *DASH714, *DASH715, *DASH716, *DASH717, *DASH718, *DASH719, *DASH720,
C *DASH721, *DASH722, *DASH723, *DASH724, *DASH725, *DASH726, *DASH727, *DASH728, *DASH729, *DASH730,
C *DASH731, *DASH732, *DASH733, *DASH734, *DASH735, *DASH736, *DASH737, *DASH738, *DASH739, *DASH740,
C *DASH741, *DASH742, *DASH743, *DASH744, *DASH745, *DASH746, *DASH747, *DASH748, *DASH749, *DASH750,
C *DASH751, *DASH752, *DASH753, *DASH754, *DASH755, *DASH756, *DASH757, *DASH758, *DASH759, *DASH760,
C *DASH761, *DASH762, *DASH763, *DASH764, *DASH765, *DASH766, *DASH767, *DASH768, *DASH769, *DASH770,
C *DASH771, *DASH772, *DASH773, *DASH774, *DASH775, *DASH776, *DASH777, *DASH778, *DASH779, *DASH780,
C *DASH781, *DASH782, *DASH783, *DASH784, *DASH785, *DASH786, *DASH787, *DASH788, *DASH789, *DASH790,
C *DASH791, *DASH792, *DASH793, *DASH794, *DASH795, *DASH796, *DASH797, *DASH798, *DASH799, *DASH800,
C *DASH801, *DASH802, *DASH803, *DASH804, *DASH805, *DASH806, *DASH807, *DASH808, *DASH809, *DASH810,
C *DASH811, *DASH812, *DASH813, *DASH814, *DASH815, *DASH816, *DASH817, *DASH818, *DASH819, *DASH820,
C *DASH821, *DASH822, *DASH823, *DASH824, *DASH825, *DASH826, *DASH827, *DASH828, *DASH829, *DASH830,
C *DASH831, *DASH832, *DASH833, *DASH834, *DASH835, *DASH836, *DASH837, *DASH838, *DASH839, *DASH840,
C *DASH841, *DASH842, *DASH843, *DASH844, *DASH845, *DASH846, *DASH847, *DASH848, *DASH849, *DASH850,
C *DASH851, *DASH852, *DASH853, *DASH854, *DASH855, *DASH856, *DASH857, *DASH858, *DASH859, *DASH860,
C *DASH861, *DASH862, *DASH863, *DASH864, *DASH865, *DASH866, *DASH867, *DASH868, *DASH869, *DASH870,
C *DASH871, *DASH872, *DASH873, *DASH874, *DASH875, *DASH876, *DASH877, *DASH878, *DASH879, *DASH880,
C *DASH881, *DASH882, *DASH883, *DASH884, *DASH885, *DASH886, *DASH887, *DASH888, *DASH889, *DASH890,
C *DASH891, *DASH892, *DASH893, *DASH894, *DASH895, *DASH896, *DASH897, *DASH898, *DASH899, *DASH900,
C *DASH901, *DASH902, *DASH903, *DASH904, *DASH905, *DASH906, *DASH907, *DASH908, *DASH909, *DASH910,
C *DASH911, *DASH912, *DASH913, *DASH914, *DASH915, *DASH916, *DASH917, *DASH918, *DASH919, *DASH920,
C *DASH921, *DASH922, *DASH923, *DASH924, *DASH925, *DASH926, *DASH927, *DASH928, *DASH929, *DASH930,
C *DASH931, *DASH932, *DASH933, *DASH934, *DASH935, *DASH936, *DASH937, *DASH938, *DASH939, *DASH940,
C *DASH941, *DASH942, *DASH943, *DASH944, *DASH945, *DASH946, *DASH947, *DASH948, *DASH949, *DASH950,
C *DASH951, *DASH952, *DASH953, *DASH954, *DASH955, *DASH956, *DASH957, *DASH958, *DASH959, *DASH960,
C *DASH961, *DASH962, *DASH963, *DASH964, *DASH965, *DASH966, *DASH967, *DASH968, *DASH969, *DASH970,
C *DASH971, *DASH972, *DASH973, *DASH974, *DASH975, *DASH976, *DASH977, *DASH978, *DASH979, *DASH980,
C *DASH981, *DASH982, *DASH983, *DASH984, *DASH985, *DASH986, *DASH987, *DASH988, *DASH989, *DASH990,
C *DASH991, *DASH992, *DASH993, *DASH994, *DASH995, *DASH996, *DASH997, *DASH998, *DASH999, *DASH1000,

```


Appendix B
Computer Plots

PARAMETER RANGE 0.000 TO 15.004



- 0.000
- 0.004
- 0.007
- 0.011
- 0.015
- 0.022
- 0.026
- 0.030
- 0.034
- 0.037
- 0.041
- 0.045
- 0.049
- 0.053
- 0.056
- 0.059
- 0.064
- 0.067
- 0.071
- 0.075
- 0.079
- 0.082
- 0.086
- 0.090
- 0.094
- 0.097
- 0.101
- 0.105
- 0.109
- 0.112
- 0.116
- 0.120
- 0.124
- 0.127
- 0.131
- 0.135
- 0.139
- 0.142
- 0.146
- 0.150

PARAMETER PAIGE 0.000 TO 18.005

PARAMETER	0.000	0.015	0.030	0.045	0.060	0.075	0.090	0.105	0.120	0.135	0.150	0.165	0.180
C.000													
C.004													
C.007													
C.011													
C.015													
C.019													
C.022													
C.026													
C.030													
C.034													
C.037													
C.041													
C.045													
C.049													
C.052													
C.056													
C.060													
C.064													
C.067													
C.071													
C.075													
C.079													
C.082													
C.086													
C.090													
C.094													
C.097													
C.101													
C.105													
C.109													
C.112													
C.116													
C.120													
C.124													
C.127													
C.131													
C.135													
C.139													
C.142													
C.146													
C.150													

PARAMETER	VALUE	UNIT	DESCRIPTION
C.000	1.000		
C.004	0.000		
C.007	0.000		
C.011	0.000		
C.015	0.000		
C.019	0.000		
C.022	0.000		
C.026	0.000		
C.030	0.000		
C.034	0.000		
C.037	0.000		
C.041	0.000		
C.045	0.000		
C.049	0.000		
C.052	0.000		
C.056	0.000		
C.060	0.000		
C.064	0.000		
C.067	0.000		
C.071	0.000		
C.075	0.000		
C.079	0.000		
C.082	0.000		
C.086	0.000		
C.090	0.000		
C.094	0.000		
C.097	0.000		
C.101	0.000		
C.105	0.000		
C.109	0.000		
C.112	0.000		
C.116	0.000		
C.120	0.000		
C.124	0.000		
C.127	0.000		
C.131	0.000		
C.135	0.000		
C.139	0.000		
C.142	0.000		
C.145	0.000		
C.150	0.000		

PARAMETER RANGE 0.000 TC 20.642

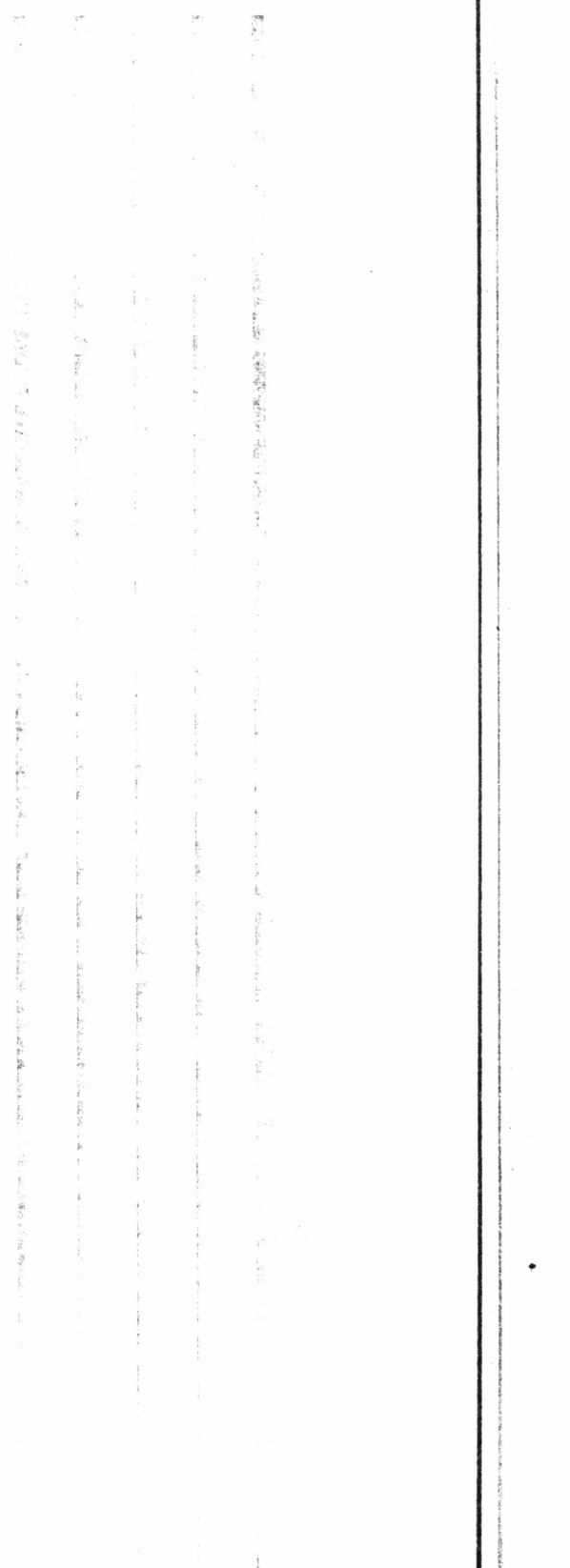
PARAMETER	RANGE	TC	20.642
C.000	0.000	20.642	0.000
C.004	0.000	20.642	0.000
G.007	0.000	20.642	0.000
O.011	0.000	20.642	0.000
O.015	0.000	20.642	0.000
C.019	0.000	20.642	0.000
O.022	0.000	20.642	0.000
C.026	0.000	20.642	0.000
O.030	0.000	20.642	0.000
O.034	0.000	20.642	0.000
O.037	0.000	20.642	0.000
O.041	0.000	20.642	0.000
S.045	0.000	20.642	0.000
O.048	0.000	20.642	0.000
O.052	0.000	20.642	0.000
C.055	0.000	20.642	0.000
C.059	0.000	20.642	0.000
O.063	0.000	20.642	0.000
C.067	0.000	20.642	0.000
O.071	0.000	20.642	0.000
O.075	0.000	20.642	0.000
C.079	0.000	20.642	0.000
O.082	0.000	20.642	0.000
C.086	0.000	20.642	0.000
O.090	0.000	20.642	0.000
O.094	0.000	20.642	0.000
C.097	0.000	20.642	0.000
O.101	0.000	20.642	0.000
C.105	0.000	20.642	0.000
O.109	0.000	20.642	0.000
O.113	0.000	20.642	0.000
C.117	0.000	20.642	0.000
O.121	0.000	20.642	0.000
C.125	0.000	20.642	0.000
O.129	0.000	20.642	0.000
C.133	0.000	20.642	0.000
O.137	0.000	20.642	0.000
C.141	0.000	20.642	0.000
O.145	0.000	20.642	0.000
C.149	0.000	20.642	0.000
O.153	0.000	20.642	0.000

Address	Value	Address	Value	Address	Value
C.000		C.004		C.008	
C.001		C.005		C.009	
C.002		C.006		C.010	
C.003		C.007		C.011	
C.004		C.008		C.012	
C.005		C.009		C.013	
C.006		C.010		C.014	
C.007		C.011		C.015	
C.008		C.012		C.016	
C.009		C.013		C.017	
C.010		C.014		C.018	
C.011		C.015		C.019	
C.012		C.016		C.020	
C.013		C.017		C.021	
C.014		C.018		C.022	
C.015		C.019		C.023	
C.016		C.020		C.024	
C.017		C.021		C.025	
C.018		C.022		C.026	
C.019		C.023		C.027	
C.020		C.024		C.028	
C.021		C.025		C.029	
C.022		C.026		C.030	
C.023		C.027		C.031	
C.024		C.028		C.032	
C.025		C.029		C.033	
C.026		C.030		C.034	
C.027		C.031		C.035	
C.028		C.032		C.036	
C.029		C.033		C.037	
C.030		C.034		C.038	
C.031		C.035		C.039	
C.032		C.036		C.040	
C.033		C.037		C.041	
C.034		C.038		C.042	
C.035		C.039		C.043	
C.036		C.040		C.044	
C.037		C.041		C.045	
C.038		C.042		C.046	
C.039		C.043		C.047	
C.040		C.044		C.048	
C.041		C.045		C.049	
C.042		C.046		C.050	
C.043		C.047		C.051	
C.044		C.048		C.052	
C.045		C.049		C.053	
C.046		C.050		C.054	
C.047		C.051		C.055	
C.048		C.052		C.056	
C.049		C.053		C.057	
C.050		C.054		C.058	
C.051		C.055		C.059	
C.052		C.056		C.060	
C.053		C.057		C.061	
C.054		C.058		C.062	
C.055		C.059		C.063	
C.056		C.060		C.064	
C.057		C.061		C.065	
C.058		C.062		C.066	
C.059		C.063		C.067	
C.060		C.064		C.068	
C.061		C.065		C.069	
C.062		C.066		C.070	
C.063		C.067		C.071	
C.064		C.068		C.072	
C.065		C.069		C.073	
C.066		C.070		C.074	
C.067		C.071		C.075	
C.068		C.072		C.076	
C.069		C.073		C.077	
C.070		C.074		C.078	
C.071		C.075		C.079	
C.072		C.076		C.080	
C.073		C.077		C.081	
C.074		C.078		C.082	
C.075		C.079		C.083	
C.076		C.080		C.084	
C.077		C.081		C.085	
C.078		C.082		C.086	
C.079		C.083		C.087	
C.080		C.084		C.088	
C.081		C.085		C.089	
C.082		C.086		C.090	
C.083		C.087		C.091	
C.084		C.088		C.092	
C.085		C.089		C.093	
C.086		C.090		C.094	
C.087		C.091		C.095	
C.088		C.092		C.096	
C.089		C.093		C.097	
C.090		C.094		C.098	
C.091		C.095		C.099	
C.092		C.096		C.100	
C.093		C.097		C.101	
C.094		C.098		C.102	
C.095		C.099		C.103	
C.096		C.100		C.104	
C.097		C.101		C.105	
C.098		C.102		C.106	
C.099		C.103		C.107	
C.100		C.104		C.108	
C.101		C.105		C.109	
C.102		C.106		C.110	
C.103		C.107		C.111	
C.104		C.108		C.112	
C.105		C.109		C.113	
C.106		C.110		C.114	
C.107		C.111		C.115	
C.108		C.112		C.116	
C.109		C.113		C.117	
C.110		C.114		C.118	
C.111		C.115		C.119	
C.112		C.116		C.120	
C.113		C.117		C.121	
C.114		C.118		C.122	
C.115		C.119		C.123	
C.116		C.120		C.124	
C.117		C.121		C.125	
C.118		C.122		C.126	
C.119		C.123		C.127	
C.120		C.124		C.128	
C.121		C.125		C.129	
C.122		C.126		C.130	
C.123		C.127		C.131	
C.124		C.128		C.132	
C.125		C.129		C.133	
C.126		C.130		C.134	
C.127		C.131		C.135	
C.128		C.132		C.136	
C.129		C.133		C.137	
C.130		C.134		C.138	
C.131		C.135		C.139	
C.132		C.136		C.140	
C.133		C.137		C.141	
C.134		C.138		C.142	
C.135		C.139		C.143	
C.136		C.140		C.144	
C.137		C.141		C.145	
C.138		C.142		C.146	
C.139		C.143		C.147	
C.140		C.144		C.148	
C.141		C.145		C.149	
C.142		C.146		C.150	

PARAMETER RANGE 0.100 TC 22.344

PARAMETER	RANGE	UNIT	VALUE
C.000	0.000		
C.004	0.007		
C.011	0.011		
C.015	0.015		
C.022	0.022		
C.026	0.026		
C.030	0.030		
C.034	0.034		
C.037	0.037		
C.041	0.041		
C.045	0.045		
C.047	0.047		
C.052	0.052		
C.056	0.056		
C.060	0.060		
C.064	0.064		
C.067	0.067		
C.071	0.071		
C.075	0.075		
C.079	0.079		
C.082	0.082		
C.086	0.086		
C.090	0.090		
C.094	0.094		
C.097	0.097		
C.101	0.101		
C.105	0.105		
C.109	0.109		
C.112	0.112		
C.116	0.116		
C.120	0.120		
C.124	0.124		
C.127	0.127		
C.131	0.131		
C.135	0.135		
C.139	0.139		
C.142	0.142		
C.146	0.146		
C.150	0.150		

Time	Value
0.000	
0.007	
0.011	
0.015	
0.019	
0.022	
0.026	
0.030	
0.034	
0.037	
0.041	
0.045	
0.049	
0.052	
0.056	
0.060	
0.064	
0.067	
0.071	
0.075	
0.079	
0.082	
0.086	
0.090	
0.094	
0.097	
0.101	
0.105	
0.109	
0.112	
0.116	
0.120	
0.124	
0.127	
0.131	
0.135	
0.139	
0.142	
0.146	
0.150	



PREPARED BY: [Illegible]

DATE: [Illegible]

TIME: [Illegible]

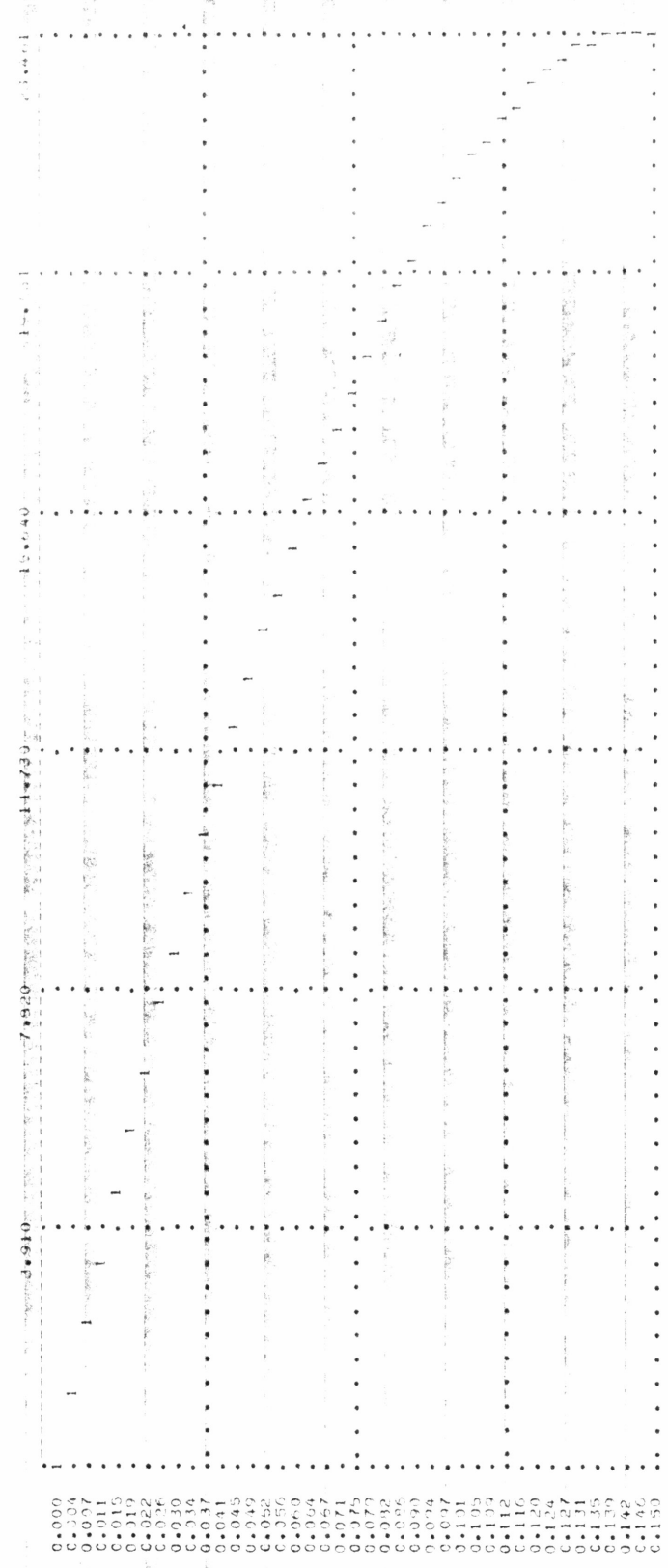
LOCATION: [Illegible]

PROJECT: [Illegible]

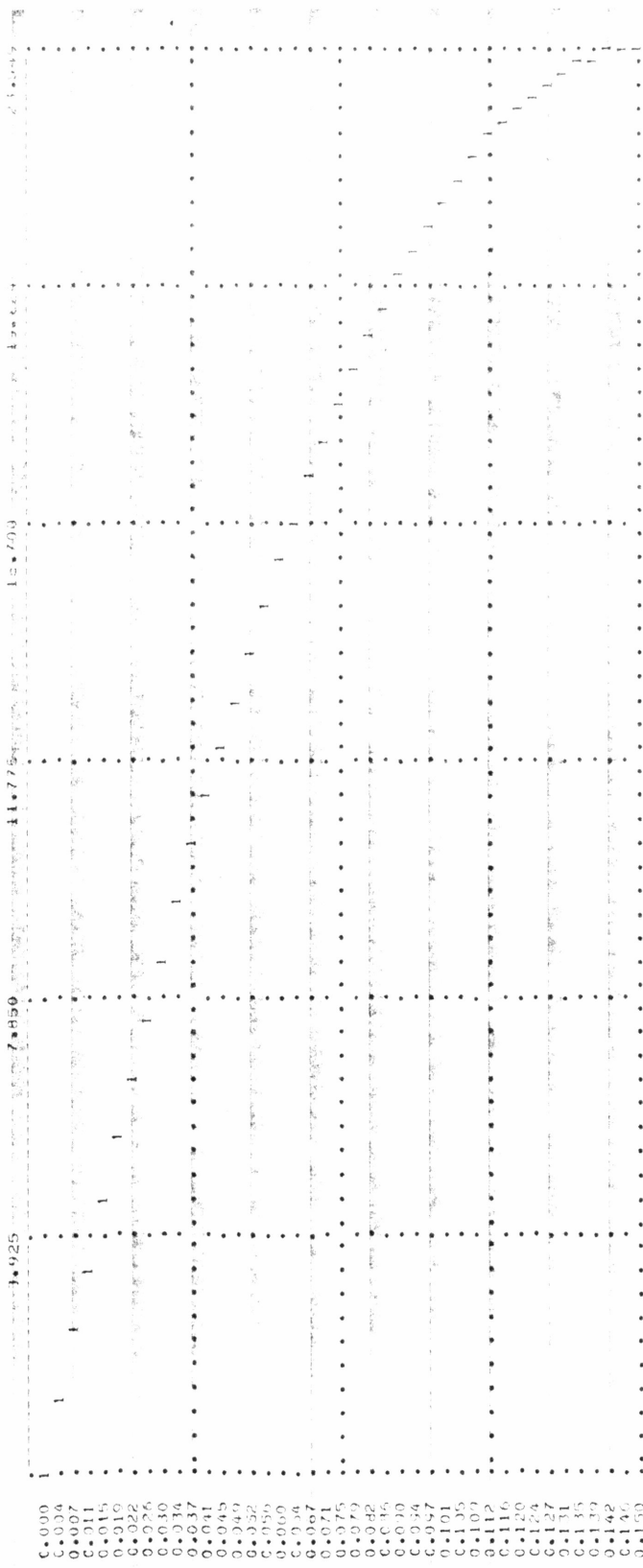
PAPAMETER RATE 0.000 TC 23.003

0.000	1	34840	11.531	15.375	23.003
0.004					
0.007					
0.011					
0.015	1				
0.019					
0.022					
0.026					
0.030					
0.034					
0.037					
0.041					
0.045					
0.049					
0.052					
0.056					
0.060					
0.064					
0.067					
0.071					
0.075					
0.079					
0.082					
0.086					
0.090					
0.094					
0.097					
0.101					
0.105					
0.109					
0.112					
0.116					
0.120					
0.124					
0.127					
0.131					
0.135					
0.139					
0.142					
0.146					
0.150					

PARAMETER DATE 0.000 IC 21.061



PARAMETER RANGE 0.000 TC 23.535



CCRE USAGE OBJECT CODE= 1498 BYTES,AMPAY AREA= 25156 BYTES, TOTAL AREA AVAILABLE= 91135 BYTES
 DIAGNOSTICS NUMBER OF LPROBS= 0, NUMBER OF WARNINGS= 0, NUMBER OF EXTENSIBLES= 0
 COMPILE TIME= 0.16 SEC, EXECUTION TIME= 5.57 SEC, 13.2885 HOURS, 20 APR 1977, 14.44, JOB 1477 VILL

//STOP